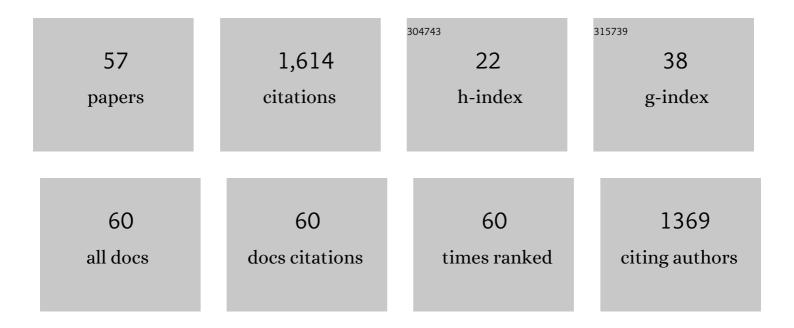
Leonardo M Angelone

List of Publications by Year in descending order

Source: https://exaly.com/author-pdf/2924202/publications.pdf Version: 2024-02-01



#	Article	IF	CITATIONS
1	MIDA: A Multimodal Imaging-Based Detailed Anatomical Model of the Human Head and Neck. PLoS ONE, 2015, 10, e0124126.	2.5	220
2	Multimodal integration of high-resolution EEG and functional magnetic resonance imaging data: a simulation study. NeuroImage, 2003, 19, 1-15.	4.2	126
3	RF-induced heating in tissue near bilateral DBS implants during MRI at 1.5â€T and 3T: The role of surgical lead management. NeuroImage, 2019, 184, 566-576.	4.2	92
4	Local <scp>SAR</scp> near deep brain stimulation (<scp>DBS</scp>) electrodes at 64 and 127 <scp>MH</scp> z: A simulation study of the effect of extracranial loops. Magnetic Resonance in Medicine, 2017, 78, 1558-1565.	3.0	81
5	Metallic electrodes and leads in simultaneous EEC-MRI: Specific absorption rate (SAR) simulation studies. Bioelectromagnetics, 2004, 25, 285-295.	1.6	74
6	Feasibility of using linearly polarized rotating birdcage transmitters and close-fitting receive arrays in MRI to reduce SAR in the vicinity of deep brain simulation implants. Magnetic Resonance in Medicine, 2017, 77, 1701-1712.	3.0	70
7	MRI-based anatomical model of the human head for specific absorption rate mapping. Medical and Biological Engineering and Computing, 2008, 46, 1239-1251.	2.8	69
8	Specific absorption rate studies of the parallel transmission of innerâ€volume excitations at 7T. Journal of Magnetic Resonance Imaging, 2008, 28, 1005-1018.	3.4	67
9	A Novel Brain Stimulation Technology Provides Compatibility with MRI. Scientific Reports, 2015, 5, 9805.	3.3	61
10	EEC/(f)MRI measurements at 7ÂTesla using a new EEG cap ("InkCapâ€). NeuroImage, 2006, 33, 1082-1092.	4.2	59
11	Construction and modeling of a reconfigurable MRI coil for lowering SAR in patients with deep brain stimulation implants. NeuroImage, 2017, 147, 577-588.	4.2	58
12	Multimodal integration of EEG and MEG data: A simulation study with variable signal-to-noise ratio and number of sensors. Human Brain Mapping, 2004, 22, 52-62.	3.6	51
13	On the effect of resistive EEG electrodes and leads during 7 T MRI: simulation and temperature measurement studies. Magnetic Resonance Imaging, 2006, 24, 801-812.	1.8	51
14	Analysis of the Role of Lead Resistivity in Specific Absorption Rate for Deep Brain Stimulator Leads at 3T MRI. IEEE Transactions on Medical Imaging, 2010, 29, 1029-1038.	8.9	46
15	Reducing RF-Induced Heating Near Implanted Leads Through High-Dielectric Capacitive Bleeding of Current (CBLOC). IEEE Transactions on Microwave Theory and Techniques, 2019, 67, 1265-1273.	4.6	46
16	Changes in the specific absorption rate (SAR) of radiofrequency energy in patients with retained cardiac leads during MRI at 1.5T and 3T. Magnetic Resonance in Medicine, 2019, 81, 653-669.	3.0	42
17	Retrospective analysis of <scp>RF</scp> heating measurements of passive medical implants. Magnetic Resonance in Medicine, 2018, 80, 2726-2730.	3.0	37
18	Assessing the Electromagnetic Fields Generated By a Radiofrequency MRI Body Coil at 64 MHz: Defeaturing Versus Accuracy. IEEE Transactions on Biomedical Engineering, 2016, 63, 1591-1601.	4.2	35

LEONARDO M ANGELONE

#	Article	IF	CITATIONS
19	The Role of Computational Modeling and Simulation in the Total Product Life Cycle of Peripheral Vascular Devices. Journal of Medical Devices, Transactions of the ASME, 2017, 11, .	0.7	35
20	Realistic modeling of deep brain stimulation implants for electromagnetic MRI safety studies. Physics in Medicine and Biology, 2018, 63, 095015.	3.0	27
21	Radio-Frequency Safety Assessment of Stents in Blood Vessels During Magnetic Resonance Imaging. Frontiers in Physiology, 2018, 9, 1439.	2.8	26
22	Parallel transmission to reduce absorbed power around deep brain stimulation devices in MRI: Impact of number and arrangement of transmit channels. Magnetic Resonance in Medicine, 2020, 83, 299-311.	3.0	25
23	MRI-Based Multiscale Model for Electromagnetic Analysis in the Human Head with Implanted DBS. Computational and Mathematical Methods in Medicine, 2013, 2013, 1-12.	1.3	22
24	On the Measurement of Electrical Impedance Spectroscopy (EIS) of the Human Head. International Journal of Bioelectromagnetism, 2010, 12, 32-46.	0.0	17
25	Computational Electromagnetic Analysis in a Human Head Model with EEG Electrodes and Leads Exposed to RF-Field Sources at 915 MHz and 1748 MHz. Radiation Research, 2010, 174, 91-100.	1.5	15
26	A numerical investigation on the effect of <scp>RF</scp> coil feed variability on global and local electromagnetic field exposure in human body models at 64 <scp>MH</scp> z. Magnetic Resonance in Medicine, 2018, 79, 1135-1144.	3.0	15
27	Investigation of assumptions underlying current safety guidelines on EM-induced nerve stimulation. Physics in Medicine and Biology, 2016, 61, 4466-4478.	3.0	14
28	A Novel Method to Decrease Electric Field and SAR Using an External High Dielectric Sleeve at 3 T Head MRI: Numerical and Experimental Results. IEEE Transactions on Biomedical Engineering, 2015, 62, 1063-1069.	4.2	13
29	Numerical and Experimental Analysis of Radiofrequency-Induced Heating Versus Lead Conductivity During EEG-MRI at 3 T. IEEE Transactions on Electromagnetic Compatibility, 2019, 61, 852-859.	2.2	12
30	Investigation of RF-Induced Heating Near Interventional Catheters at 1.5 T MRI: A Combined Modeling and Experimental Study. IEEE Transactions on Electromagnetic Compatibility, 2019, 61, 1423-1431.	2.2	11
31	The â€~virtual DBS population': five realistic computational models of deep brain stimulation patients for electromagnetic MR safety studies. Physics in Medicine and Biology, 2019, 64, 035021.	3.0	11
32	A Study on the Feasibility of the Deep Brain Stimulation (DBS) Electrode Localization Based on Scalp Electric Potential Recordings. Frontiers in Physiology, 2019, 9, 1788.	2.8	10
33	Specific absorption rate in a standard phantom containing a Deep Brain Stimulation lead at 3 Tesla MRI. , 2013, , .		8
34	fMRI Priors for the Linear Inverse Estimation of EEG Cortical Sources. Electromagnetics, 2001, 21, 579-592.	0.7	7
35	High dielectric material in MRI: Numerical assessment of the reduction of the induced local power on implanted cardiac leads. , 2016, 2016, 2361-2364.		7
36	A computational model for bipolar deep brain stimulation of the subthalamic nucleus. , 2014, 2014,		6

6258-61.

#	Article	IF	CITATIONS
37	Effects of tuning conditions on near field of MRI transmit birdcage coil at 64 MHz. , 2016, 2016, 6242-6245.		6
38	A Virtual Patient Simulator Based on Human Connectome and 7 T MRI for Deep Brain Stimulation. International Journal on Advances in Life Sciences, 2014, 6, 364-372.	1.0	6
39	RF Safety Evaluation of a Breast Tissue Expander Device for MRI: Numerical Simulation and Experiment. IEEE Transactions on Electromagnetic Compatibility, 2017, 59, 1390-1399.	2.2	5
40	Improvement of Electromagnetic Field Distributions Using High Dielectric Constant (HDC) Materials for CTL-Spine MRI: Numerical Simulations and Experiments. IEEE Transactions on Electromagnetic Compatibility, 2017, 59, 1382-1389.	2.2	5
41	Computational platform combining detailed and precise functionalized anatomical phantoms with EM-Neuron interaction modeling. , 2014, , .		4
42	Analysis of Conservative and Magnetically Induced Electric Fields in a Low-Frequency Birdcage Coil. Journal of Electromagnetic Analysis and Applications, 2013, 05, 271-280.	0.2	4
43	Effect of Multiple Scattering on Heating Induced by Radio Frequency Energy. IEEE Transactions on Electromagnetic Compatibility, 2020, 62, 2311-2316.	2.2	3
44	Real Time MR Thermometry Using Tm-DOTMA. Journal of Electromagnetic Analysis and Applications, 2015, 07, 115-125.	0.2	3
45	Assessment of MRI Issues at 7 T. American Journal of Roentgenology, 2014, 203, W560-W560.	2.2	2
46	RF induced energy for partially implanted catheters: A computational study. , 2016, 2016, 1256-1259.		2
47	Investigating the effect of coil model losses on computational electromagnetic exposure of an ASTM phantom at 64 MHz MRI. , 2017, 2017, 1481-1484.		2
48	Multimodal integration of high resolution EEG and functional magnetic resonance: a simulation study. NeuroImage, 2001, 13, 66.	4.2	1
49	Evaluation of unintended electrical stimulation from MR gradient fields. Frontiers in Bioscience - Elite, 2012, E4, 1731.	1.8	1
50	A New Method to Concentrate Electromagnetic Field Within ROI Using a High Dielectric Material in 3T Body MRI. , 2013, , .		1
51	Simulation platform for coupled modeling of EM-induced neuronal dynamics and functionalized anatomical models. , 2015, , .		1
52	Computational assessment of radiofrequency energy absorption of fetus during an MRI scan. Biomedical Physics and Engineering Express, 2018, 4, 045032.	1.2	1
53	Multimodal integration of high resolution EEG and functional magnetic resonance: a simulation study. , 0, , .		0
54	A Novel Method to Decrease Electric Field and SAR Using an External High Dielectric Sleeve at 3T Head MRI: Numerical and Experimental Results. , 2013, , .		0

#	Article	IF	CITATIONS
55	The electromagnetic fields of a 64 MHz quadrature driven birdcage coil in ASTM phantom. , 2017, , .		Ο
56	Effect Of Incident Field Magnitude And Phase Distribution On Rfinduced Heating Due To Hip Implants. , 2018, 2018, 1360-1363.		0
57	Coupled modeling and experimental investigation of RF-induced heating near ablation catheters under 1.5T MRI. , 2018, , .		0